Autophagy 8:6, 927–937; June 2012; © 2012 Landes Bioscience

Caspase activation regulates the extracellular export of autophagic vacuoles

Isabelle Sirois,[1] Jessika Groleau,[1] Nicolas Pallet,[1] Nathalie Brassard,[1] Katia Hamelin,[1] Irène Londono,[3] Alexey V. Pshezhetsky,[2] Moïse Bendayan[3,†] and Marie-Josée Hébert[1†,*]

[1]Research Centre; Centre Hospitalier de l'Université de Montréal (CRCHUM); Montréal, Canada; [2]Research Centre; Centre Hospitalier Universitaire Sainte-Justine; Montréal, Canada; [3]Department of Pathology and Cell Biology; Faculty of Medicine; Université de Montréal, Centreville; Montréal, Canada

[†]These authors contributed equally to this work.

Keywords: nutrient deprivation, autophagic vacuoles, caspase activation, unconventional secretion, autophagy, caspase-3

Abbreviations: SS, serum starvation; 2D-LC-MS/MS, 2-dimension liquid chromatography and tandem mass spectrometry; AV, autophagic vacuoles; DMSO, dimethylsulfoxide; EC, endothelial cells; FPLC, fast protein liquid chromatography; HO, Hoechst 33342 (2'-(4-ethoxyphenyl)-5-(4-methyl-1-piperazinyl)-2.5'-bi-1H-benzimidazole; HUVEC, human umbilical vascular endothelial cells; LC3, microtubule-associated proteins 1A and 1B light chain 3; MVB, multivesicular bodies; N, normal growth medium; Nu, nucleus; PARP, poly (ADP-ribose) polymerase; PI, propidium iodide; SDS-PAGE, sodium dodecyl sulfate-polyacrylamide gel electrophoresis; SSC, serum-free medium conditioned by serum-starved EC; SSC-ZVAD, serum-free medium conditioned by serum-staved EC treated with ZVAD-FMK; TCTP, translationally-controlled tumor protein; *C3*$^{-/-}$, CASP3-deficient mice; WT, wild-type mice; Acb1, acyl co-enzyme A binding protein

The endothelium plays a central role in the regulation of vascular wall cellularity and tone by secreting an array of mediators of importance in intercellular communication. Nutrient deprivation of human endothelial cells (EC) evokes unconventional forms of secretion leading to the release of nanovesicles distinct from apoptotic bodies and bearing markers of multivesicular bodies (MVB). Nutrient deficiency is also a potent inducer of autophagy and vesicular transport pathways can be assisted by autophagy. Nutrient deficiency induced a significant and rapid increase in autophagic features, as imaged by electron microscopy and immunoblotting analysis of LC3-II/LC3-I ratios. Increased autophagic flux was confirmed by exposing serum-starved cells to bafilomycin A_1. Induction of autophagy was followed by indices of an apoptotic response, as assessed by microscopy and poly (ADP-ribose) polymerase cleavage in absence of cell membrane permeabilization indicative of necrosis. Pan-caspase inhibition with ZVAD-FMK did not prevent the development of autophagy but negatively impacted autophagic vacuole (AV) maturation. Adopting a multidimensional proteomics approach with validation by immunoblotting, we determined that nutrient-deprived EC released AV components (LC3I, LC3-II, ATG16L1 and LAMP2) whereas pan-caspase inhibition with ZVAD-FMK blocked AV release. Similarly, nutrient deprivation in aortic murine EC isolated from CASP3/caspase 3-deficient mice induced an autophagic response in absence of apoptosis and failed to prompt LC3 release. Collectively, the present results demonstrate the release of autophagic components by nutrient-deprived apoptotic human cells in absence of cell membrane permeabilization. These results also identify caspase-3 as a novel regulator of AV release.

Introduction

The endothelium plays a central role in the regulation of vascular wall cellularity and tone by secreting an array of mediators of importance in intercellular communication. Endothelial apoptosis in response to various cellular stresses either immune or nonimmune is critical to most vascular diseases. Apoptotic cells actively release membrane-bound apoptotic bodies originating from blebbing of the cell membrane.[1,2] We demonstrated recently that, in addition to membrane blebbing, unconventional forms of secretion are activated in human apoptotic endothelial cells (EC) leading to the release of nanovesicles biochemically and functionally distinct from apoptotic bodies and bearing markers of multivesicular bodies (MVB).[3] Pan-caspase inactivation or small interfering RNAs targeting CASP3 significantly reduced release of MVB components by apoptotic cells. However, release of MVB constituents was described in an experimental setting where human EC were acutely deprived of growth factors, a classical pro-apoptotic stimulus but also a potent inducer of autophagy.

During autophagy, autophagosome formation begins with the isolation of autophagic cargo through membrane-wrapping of cytoplasmic components or organelles targeted for lysosomal

*Correspondence to: Marie-Josée Hébert; Email: marie-josee.hebert.chum@ssss.gouv.qc.ca
Submitted: 07/24/11; Revised: 01/30/12; Accepted: 02/20/12
http://dx.doi.org/10.4161/auto.19768

degradation. Endoplasmic reticulum as well as plasma membranes participate in the initiation of autophagosome formation.[4] Immunoelectron microscopy as well as endocytic tracers and lysosomal markers have identified various maturation stages of autophagic vacuoles (AV), reflecting the dynamic nature of the autophagic program.[5,6] Immature AV contain intact cytoplasmic portions or organelles delimited by multiple membranes with areas of electron-lucent material. Further maturation is associated with the presence of heterogenic electron-opaque material and/or multilamellar lysosomal bodies demonstrating lysosome-autophagosome interactions leading to protein degradation. Fusion between autophagosomes and MVB leading to the formation of amphisomes has been described.[5,7-9] Amphisomes are characterized by the presence of both electron-dense autophagosome constituents with a delimiting membrane and MVB nanovesicular content.[6,10] Collectively, these results suggest that during their formation and maturation, AV interact dynamically with various intracellular compartments. Although classically considered degradation devices destined to fuse with lysosomes, recent results in yeast have highlighted the possibility that autophagosomes may fail to fuse with lysosomes and instead be released into the extracellular milieu.[11,12]

In the present work, we evaluated whether human cells can also release AV and whether caspase activation regulates this pathway. Several cues prompted us to evaluate the importance of caspases in extracellular export of AV components in eukaryotes. Caspase activation and more specifically activation of the effector caspase-3 has been implicated in the orchestration of a finely regulated paracrine response leading to the release of protein and lipid mediators of importance in tissue remodeling at sites of cell deletion.[1-3,13-15] Nonclassical secretion pathways involving at least in part the release of MVB components in absence of cell membrane permeabilization has been described downstream of caspase-3 activation.[3] Therefore, the mainstay of this study was to characterize AV export pathways and to assess the importance of caspase activation for their release in the extracellular milieu.

Results

SS concomitantly induces apoptotic and autophagic features in human EC. We showed previously that nutrient deprivation associated with serum starvation (SS) sequentially activates CASP9/caspase 9 in human EC, leading to caspase-dependent apoptotic cell death.[3] SS is also a classical pro-autophagic stimulus. Here, we first aimed at characterizing the kinetics of apoptosis and autophagy in response to SS. Electron and fluorescence microscopy with Hoechst 33342 (HO) and propidium iodide (PI) demonstrated that, in serum-starved EC, the percentage of cells showing nuclear condensation characteristic of apoptosis increased significantly over 4 h (**Fig. 1A–C**). Chromatin condensation developed in the absence of cell membrane permeabilization, demonstrating that primary and secondary necrotic features were not activated in response to SS for 4 h (**Fig. 1C**). Cleavage of the caspase-3 substrate Poly(ADP-ribose) polymerase (PARP) corroborated the morphological nuclear findings apparent in EC serum starved for 3 h and persisted thereafter (**Fig. 1D**), confirming effector caspases activation.

We then examined the kinetics of autophagy in this system. LC3-II/LC3-I ratios increased significantly in EC serum starved for 2 h. This heightened ratio persisted for the entire study duration (**Fig. 1E**). Serum-starved EC exposed to bafilomycin A_1 showed accumulation of LC3-II, confirming enhanced autophagic flux in this system (**Fig. 1F**). Electron microscopy was used to further assess AV in serum-starved EC. AV at different maturation stages were identified (**Fig. 1G–K**) and the total cytoplasmic area occupied by AV increased significantly as compared with EC exposed to normal medium (N) (**Fig. 1L**). Taken together, these results confirmed that SS concomitantly induces autophagic and apoptotic programs in human EC.

Caspase inhibition does not prevent development of autophagy in serum-starved EC. To functionally address the interplay between caspase activation and autophagy during serum starvation, EC were exposed to SS in the presence of the pan-caspase inhibitor ZVAD-FMK. Caspase inhibition blocked the nuclear changes associated with apoptosis development, as evaluated by fluorescence microscopy as well as PARP cleavage (**Fig. 2A and B**). Cell membrane permeabilization did not increase significantly in the presence of ZVAD-FMK, demonstrating that caspase inhibition did not redirect cell death toward necrosis (**Fig. 2A**). Ultrastructural analysis of EC serum starved with ZVAD-FMK (SS+ZVAD) revealed increased autophagic vacuolization compared with EC incubated with SS (**Fig. 2C–G**). Morphometrical evaluation of equivalent cytoplasmic area of cell profiles in EC treated with SS or SS+ZVAD (**Fig. 2E**)

Figure 1 (See opposite page). Serum starvation (SS) in EC induces both apoptotic and autophagic features. (A and B) Electron micrographs of normal and apoptotic EC. The nucleus (Nu) of EC exposed to complete growth medium (Normal) displays an elongated aspect whereas that of serum-starved EC (SS) for 4 h appears rounded and condensed, characteristic of apoptosis. Scale bar: 1 μm. (C) Percentages of cells with increased chromatin condensation (apoptosis) and cell membrane permeabilization (necrosis), as evaluated by HO and PI staining, in EC exposed to normal medium (N) or SS for 1–4 h. *$p \leq 0.0007$ vs. N, n = 6. (D) Immunoblot for uncleaved and cleaved forms of PARP in EC treated as in (C), representative of 4 experiments. (E) Upper panel: Time-course of LC3 turnover, by immunoblot, in EC treated as in (A–D). Lower panel: Densitometry analysis of LC3-II/LC3-I ratios in EC exposed to N or SS for 1–4 h. *$p \leq 0.01$ vs. N. Representative of four experiments. (F) LC3-I and -II immunoblot in EC exposed to N, SS and SS + bafilomycin A_1 5 nM for 4 h (the immunoblot corresponds to two parts of the same gel). Representative of four experiments. (G–K) Morphological characterization of AV in EC serum starved for 4 h. (G) AV with intact cytoplasmic portions or organelles delimited by multiple membranes with internal electron-lucent material and cytoplasm. (H and I) AV with various stages of degraded cytoplasmic material, characterized by increased electron density within vacuoles surrounded by single or double delimiting membranes. (J) AV displaying a more advanced degradation stage with multilamelar lysosomal bodies (white star). (K) Amphisomes are characterized by the presence of both autophagosomal electron-dense material with a delimiting membrane and MVB nanovesicular content. Scale bar: 0.5 μm. (L) Total cytoplasmic area (μm^2) occupied by AV per cell profile in EC exposed for 4 h to N and SS, respectively. Area of AV per cell profile (n = 20) was assessed in relation to the cell cytoplasm (nuclei were not included in the evaluation); *$p \leq 0.001$ vs. N.

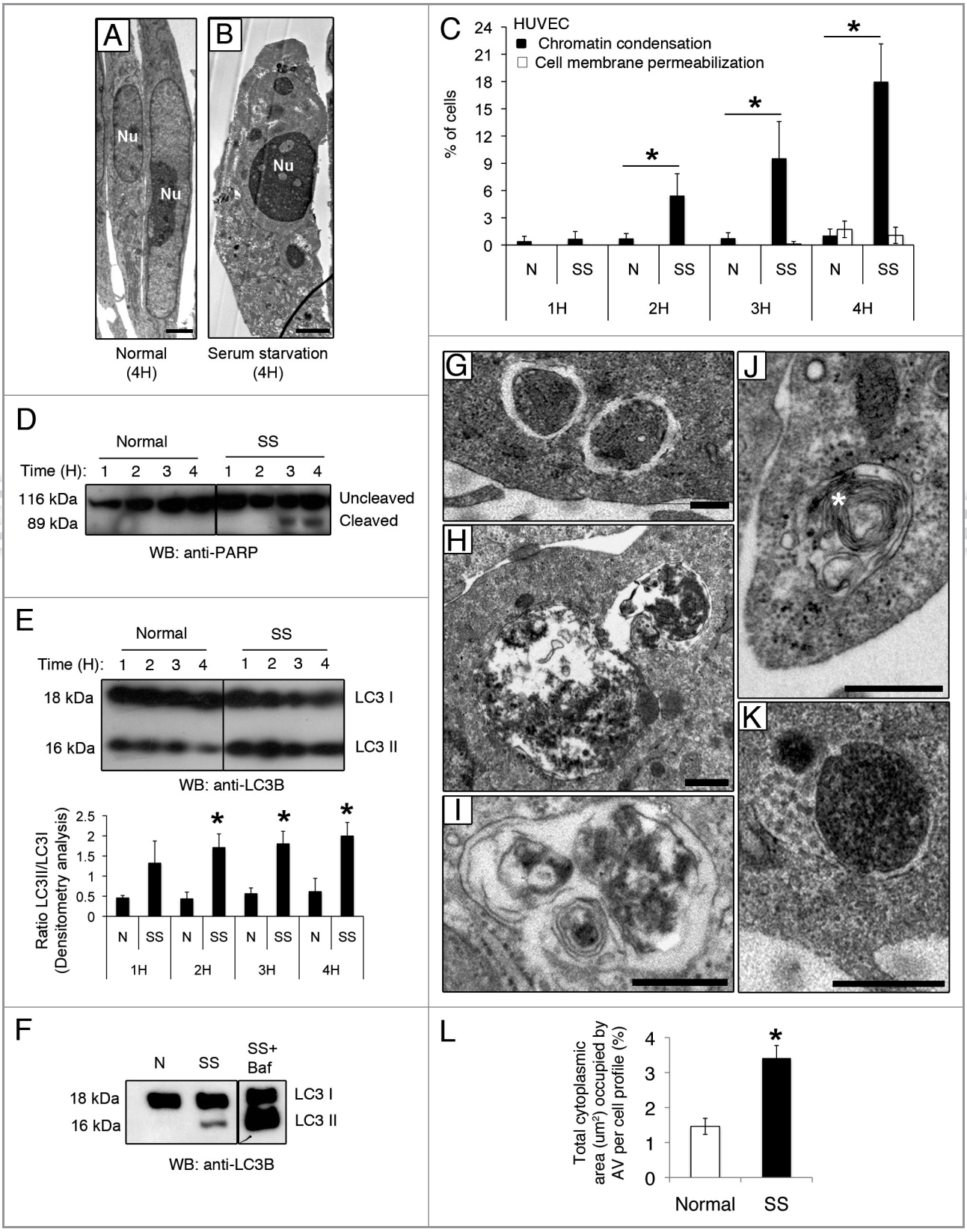

Figure 1. For figure legend, see page 928.

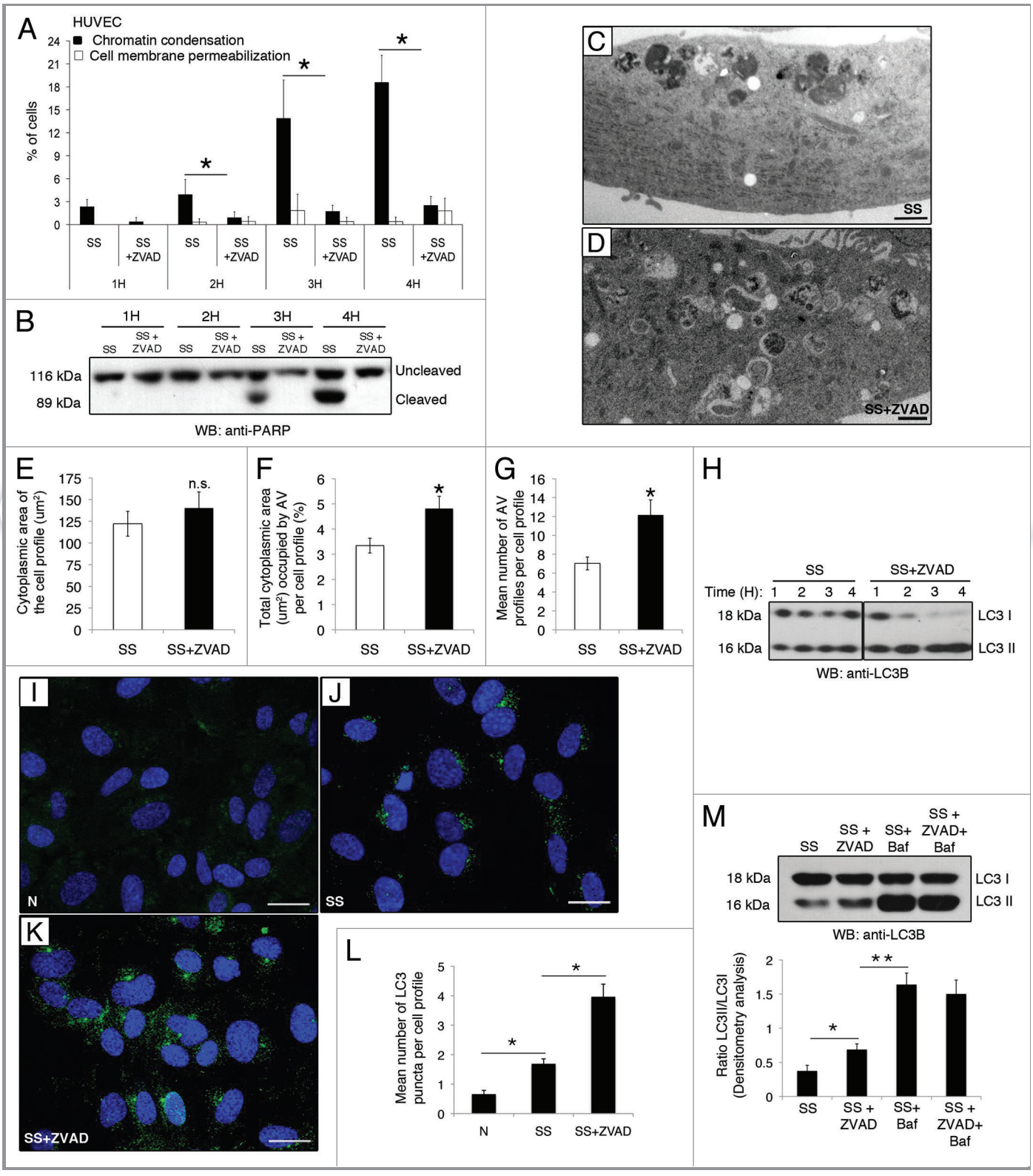

Figure 2. For figure legend, see page 931.

Figure 2 (See opposite page). Caspase inhibition does not prevent development of autophagy in serum-starved EC. (A) Percentages of cells with increased chromatin condensation (apoptosis) and cell membrane permeabilization (necrosis), as evaluated by HO and PI staining, in EC exposed to SS in presence of the pan-caspase inhibitor ZVAD-FMK (SS+ZVAD) 50 μM or SS + vehicle DMSO (SS) for 1–4 h. *p ≤ 0.002 vs. Z, n = 6. (B) Immunoblot for uncleaved and cleaved PARP in EC treated as described above. Representative of 4 experiments. (C and D) Electron micrographs of EC serum starved for 4 h with vehicle DMSO [SS, (C)] or with ZVAD-FMK 50 μM [SS+ZVAD, (D)]. Scale bar: 1 μm. (E) Mean cytoplasmic area of the cell profiles. (F) Percentage of total cytoplasmic area (μm^2) occupied by AV per cell profile in EC treated as in (A–D). *p = 0.01 vs. SS; n = 30 cell profiles. (G) Mean number of AV profiles per cell profile in EC serum starved for 4 h in presence of the pan-caspase inhibitor ZVAD-FMK 50 μM (SS+ZVAD) or vehicle DMSO (SS). *p ≤ 0.0005 and **p ≤ 0.005 vs. SS; n = 30 cell profiles. (H) Time course of LC3 turnover by immunoblot in EC treated as in A (the immunoblot corresponds to two parts of the same gel). Representative of three experiments. (I–K) Native LC3 immunostaining evaluated by confocal microscopy in EC exposed either to (I) normal medium (N) or serum-starved and treated with (J) vehicle DMSO (SS) or (K) ZVAD-FMK 50 μM (SS+ZVAD). (L) Mean number of LC3 puncta per cell profile evaluated by confocal microscopy immunostaining in EC treated as above. LC3 puncta were counted in approximatly 50 cells/representative section of the sample in three different trials; p ≤ 0.0001. (M) Upper panel: LC3-I and -II immunoblot in EC exposed to vehicule (SS), SS+ZVAD (50 μM), SS + bafilomycin A_1 (5 nM) or SS + ZVAD + bafilomycin A_1 for 4 h. Lower panel: Densitometry analysis of the LC3-II/LC3-I ratio. *p ≤ 0.02 vs. SS, **p ≤ 0.0002 vs SS+ZVAD. Representative of four experiments.

demonstrated a significant increase in total cytoplasmic area occupied by AV in serum-starved EC exposed to ZVAD-FMK (**Fig. 2F**). This change represented approximately a 2-fold increase in the mean number of AV profiles per cell profile (**Fig. 2G**). LC3-II/LC3-I ratios were further increased in serum-starved EC (SS) compared with normal medium (N) and was further increased when exposed to ZVAD-FMK (**Fig. 2H**). Similarly, the mean number of LC3 puncta per cell was increased in EC serum starved with ZVAD-FMK as compared with SS treatment alone (**Fig. 2I–L**). Collectively, these results suggest enhanced AV formation, accumulation or both in ZVAD-FMK-treated serum-starved EC. Co-incubation of serum-starved EC with ZVAD-FMK and bafilomycin A_1 did not further increase LC3-II accumulation as compared with bafilomycin A_1 alone (**Fig. 2M**), suggesting that caspase inhibition has an impact upon AV maturation but not their de novo formation.

Caspase activation impacts AV maturation. Ultrastructural analysis of serum-starved EC by electron microscopy showed accumulation of AV at different maturation stages in proximity with the cell membrane in serum-starved EC (**Fig. 3A, B and F**). Large autophagic networks composed of AV with several contact sites and containing heterogeneous material were observed (**Fig. 3B**). These large autophagic networks were seldom found in EC serum starved with ZVAD-FMK (**Fig. 3C–E**). AV contact sites, assessed quantitatively by electron microscopy (**Fig. 3F**), were significantly lower in EC serum starved with ZVAD-FMK compared with SS alone. Collectively, these results suggest a novel role for caspase activation in the regulation of AV maturation.

AV components are released through caspase-dependent pathways. Since AV accumulate in serum-starved EC upon caspase inhibition (**Fig. 2D, F and G**), we hypothesized that caspase activation could regulate the release of AV content. To test this hypothesis, we used a multidimensional and comparative proteomic approach to evaluate if AV components were released through caspase-dependent pathways in medium conditioned by serum-starved EC.[3,13,14] Briefly, equal EC numbers were exposed to either vehicle (DMSO) or ZVAD-FMK for 2 h and then serum starved for 4 h. The conditioned media (SSC and SSC-ZVAD respectively) were then sequentially centrifuged to remove cell debris and apoptotic blebs. Proteins from SSC and SSC-ZVAD were then analyzed comparatively either by two-dimensional liquid chromatography-tandem mass spectrometry (2D-LC-MS/MS) or SDS-PAGE LC-MS/MS.

The following criteria were used to assess the release of AV components by apoptotic and non-apoptotic, serum-starved EC: (1) protein previously reported to be associated with AV formation, expansion or fusion; (2) protein identified in SSC or in SSC-ZVAD only or with a significant differential abundance ratio of SSC /SSC-ZVAD greater than 2.0; and (3) protein of human origin (**Table 1**; **Table S1**). Data analysis of these secretomes revealed specific enrichment for proteins associated with AV formation and expansion (LC3, ATG4D, ATG16L1) in medium conditioned by apoptotic serum-starved EC (SSC). Proteins coupled with the fusion of autophagosomes with MVB and/or lysosomes (VPS4/SKD1, VPS16, LAMP2) were also represented predominantly in SSC (**Table 1**). The specific enrichment of LAMP2, LC3-I, LC3-II and ATG16L1 in SSC as compared with SSC-ZVAD was confirmed by immunoblotting (**Fig. 4A**). Taken together, these results confirmed that caspase activation favors extracellular export of AV components in absence of cell membrane permeabilization. AV near and/or interacting with the cell membrane were frequently identified by electron microscopy in serum-starved EC (**Fig. 4B–E**) but rarely present in EC serum starved in presence of ZVAD-FMK (**Fig. 4F and G**). The mean distance between AV and the cell membrane, evaluated by electron microscopy, was significantly increased in EC serum starved in presence of ZVAD-FMK, as compared with control EC (SS) (**Fig. 4H**). Collectively, these results suggest that caspase activation regulates AV interactions with the cell membrane.

CASP1/caspase 1 has been identified as a molecular regulator of unconventional secretion pathways and can be inhibited by ZVAD-FMK.[24] Nutrient-deprived EC did not demonstrate caspase-1 cleavage, ruling out a contribution of active caspase-1 in our system (**Fig. S1A**). Mounting evidence suggests that in plants and eukaryotic cells, caspase-3 activation fosters unconventional modes of protein secretion.[3,25] To better define the role of caspase-3 activation in the extracellular release of AV components, aortic EC from CASP3-deficient mice ($C3^{-/-}$) and wild-type (WT) controls (**Fig. S1B**) were serum starved for 4 h. As expected, serum-starved $C3^{-/-}$ EC showed resistance to apoptosis, as demonstrated by absence of nuclear changes (**Fig. 5A**). Autophagy was not inhibited in murine EC as LC3-II/LC3-I ratios tended to increase further in serum-starved $C3^{-/-}$ EC compared with WT (**Fig. 5B**). As observed in ZVAD-FMK-treated serum-starved EC (**Fig. 2F–G and H**), electron

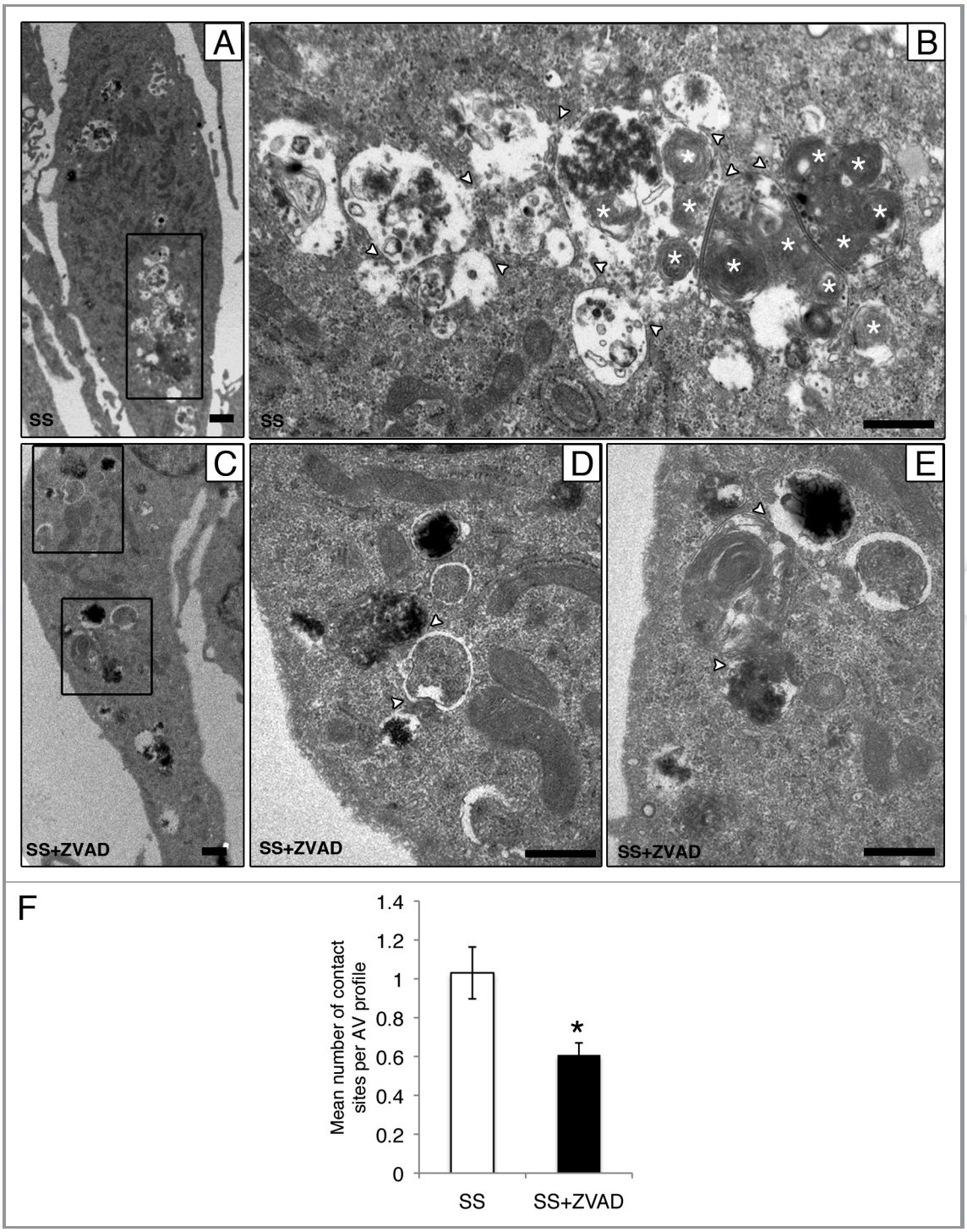

Figure 3. Caspase activation regulates the formation of autophagic network. (A–E) Electron micrographs of serum-starved EC exposed to ZVAD-FMK 50 μM (SS+ZVAD) or vehicle (SS) for 4 h. (A and B) Autophagic network (islet in A) with different maturation stages observed in serum-staved EC. Multilamellar electron-dense lysosomal bodies are also represented (white stars). White arrowheads indicate contact sites between AV. Scale bars: (A) 0.5 μm; (B) 2 μm. (C–E) Electron micrographs of EC serum starved with ZVAD-FMK 50 μM (SS+ZVAD) showing individual AV (islet in D and E) as opposed to large autophagic network seen in (B). Scale bars: (C) 0.5 μm; (D and E) 2 μm. (F) Mean number of contact sites per AV profile quantified for each condition; n = 30 cell profiles per condition; p = 0.005.

microscopy showed an increased vacuolization in serum-starved *C3*$^{-/-}$ EC (**Fig. 5F–H**) compared with WT EC (**Fig. 5C and D**). In serum-starved *C3*$^{-/-}$ EC, interactions between AV with the cell membrane were rarely observed (**Fig. 5F–H**) but present in WT controls (**Fig. 5D and E**). Also, serum-free medium conditioned by *C3*$^{-/-}$ EC showed reduced LC3-II/LC3-I levels as

Table 1. List of autophagy-related proteins identified by LC-MS-MS in media conditioned by serum-starved, caspase-activated EC (SSC) and serum-starved, caspase-inhibited EC (SSC-ZVAD)

No.	Protein identified by LC-MS-MS	Gene name	Function during autophagy
		Predominant in SSC	
1	LC3/Microtubule-associated proteins 1A/1B, light chain 3	MAP1LC3B	Autophagosome formation and expansion. Cytosolic and membrane-bound to autophagosomes.[16,17]
2	Cysteine protease ATG4D	ATG4D	Autophagosome formation and expansion. Cleaves the C-terminal part of MAP1LC3.[16,18]
3	Autophagy related protein 16-like 1	ATG16L1	Autophagosome formation and expansion. Associates with ATG12–ATG15 complex.[19]
4	VPS4 AAA ATPase/vacuolar protein sorting-associated protein 4B	VPS4/SKD1	Autophagosome formation and MVB biogenesis. Fusion of autophagosomes with endosomes and lysosomes.[6,20]
5	Vacuolar protein sorting-associated protein 16 homolog	VPS16	Formation and fusion of autolysosomes and endolysosomes.[21,22]
6	Lysosome-associated membrane glycoprotein 2	LAMP2	Fusion of autophagosomes with lysosomes.[6,23]
		Predominant in SSC-ZVAD	
1	Ras-related protein RAB7a	RAB7A	Fusion of autophagosomes and amphisomes with lysosomes.[6,37]

compared with serum-free medium conditioned by an equivalent number of WT EC (**Fig. 5I**). Collectively, these results highlight a novel role for caspase-3 in regulation of AV externalization in eukaryotic cells.

Discussion

Autophagy is classically considered a degradative process responsible for the elimination of unnecessary or defective cellular proteins and organelles. In conditions of reduced nutrient availability, autophagy allows reuse of intracellular proteins to maintain energy levels and prevents the activation of programmed death pathways. Mounting evidence suggests that the autophagic system is central for the elimination of microorganisms, tumor suppression and antigen presentation.[26] Recently, interactions between autophagosomes and MVB, leading to the extracellular export of Acb1 (*acyl co-enzyme A binding protein* lacking a secretory signal peptide) in yeast, have been described.[11,12] These results, in lower eukaryotes, indicate a novel role for the autophagic process in intercellular communication through activation of nonclassical secretion pathways. Autophagy gene products (LC3), MVB components (VPS4 and TSG101) and SNARE proteins have been shown to be essential for the unconventional secretion of Acb1 by serum-starved *D. discoideum*.[11] Vesicular transport pathways assisted by autophagy have also been demonstrated for unconventional secretion and viral replication.[27]

The present work lends further support to these recent reports and demonstrates that autophagic components are released by human EC under conditions of reduced nutrient availability in association with caspase-3 activation. We determined that serum starvation rapidly increases autophagic flux in EC. We observed that autophagy predated development of apoptosis and persisted while apoptosis was activated. Necrosis however was not activated in this system, as the percentage of cells with evidence of cell membrane permeabilization did not increase during serum starvation. Unbiased proteomic analysis and validation by western blotting confirmed the presence of several autophagic proteins in medium conditioned by serum-starved EC, including LC3 and ATG16L1.

We identified caspases, and more precisely caspase-3, as novel regulators of AV maturation and release. Proteomic analysis and validation by western blotting showed that pan-caspase inhibition prevents the release of AV components in the extracellular milieu. Also, the mean distance between AV and the cell membrane increased in presence of the pan-caspase inhibitor ZVAD-FMK. Evaluation of AV maturation and release in CASP3-deficient mice corroborated these results. Serum-starved CASP3-deficient ($C3^{-/-}$) EC failed to develop apoptotic nuclear features upon serum starvation but activated an autophagic response. However, extracellular release of LC3 was largely inhibited in $C3^{-/-}$ serum-starved EC.

Mounting evidence suggests that caspase activity regulates unconventional modes of secretion. A significant proportion of the caspase-dependent secretome of nutrient-deprived EC is composed of proteins devoid of secretion signals, indicating an association between caspase activation and unconventional secretion pathways.[3] Ultrastructural and biochemical studies have confirmed the contribution of the MVB compartment to the secretion of TCTP, a known marker of MVB and exosomes, by serum-starved EC.[3,28] Caspase-1 activation has also been identified as a novel regulator of unconventional protein secretion pathways. Activated Caspase-1 has been implicated in the export of various leaderless proteins, such as IL1A and B/interleukin-1α and β and FGF2/basic fibroblast growth factor-2, through nonconventional secretion pathways.[24] In our system, nutrient-deprived EC failed to show evidence of caspase-1 activation, ruling out a contribution of caspase-1 in AV release. Mounting evidence from our group and others suggests that caspase-3, the central death effector caspase, also plays important roles in unconventional protein and lipid secretion in plant and eukaryotic cell.[25] Caspase-3 activation in apoptotic EC elicits the secretion of a highly-regulated set of mediators of importance in tissue remodeling.[1-3,13-15] Our results show that pan-caspase inhibition or CASP3 genetic invalidation both prevents the release of AV constituents in the extracellular milieu. We and others have

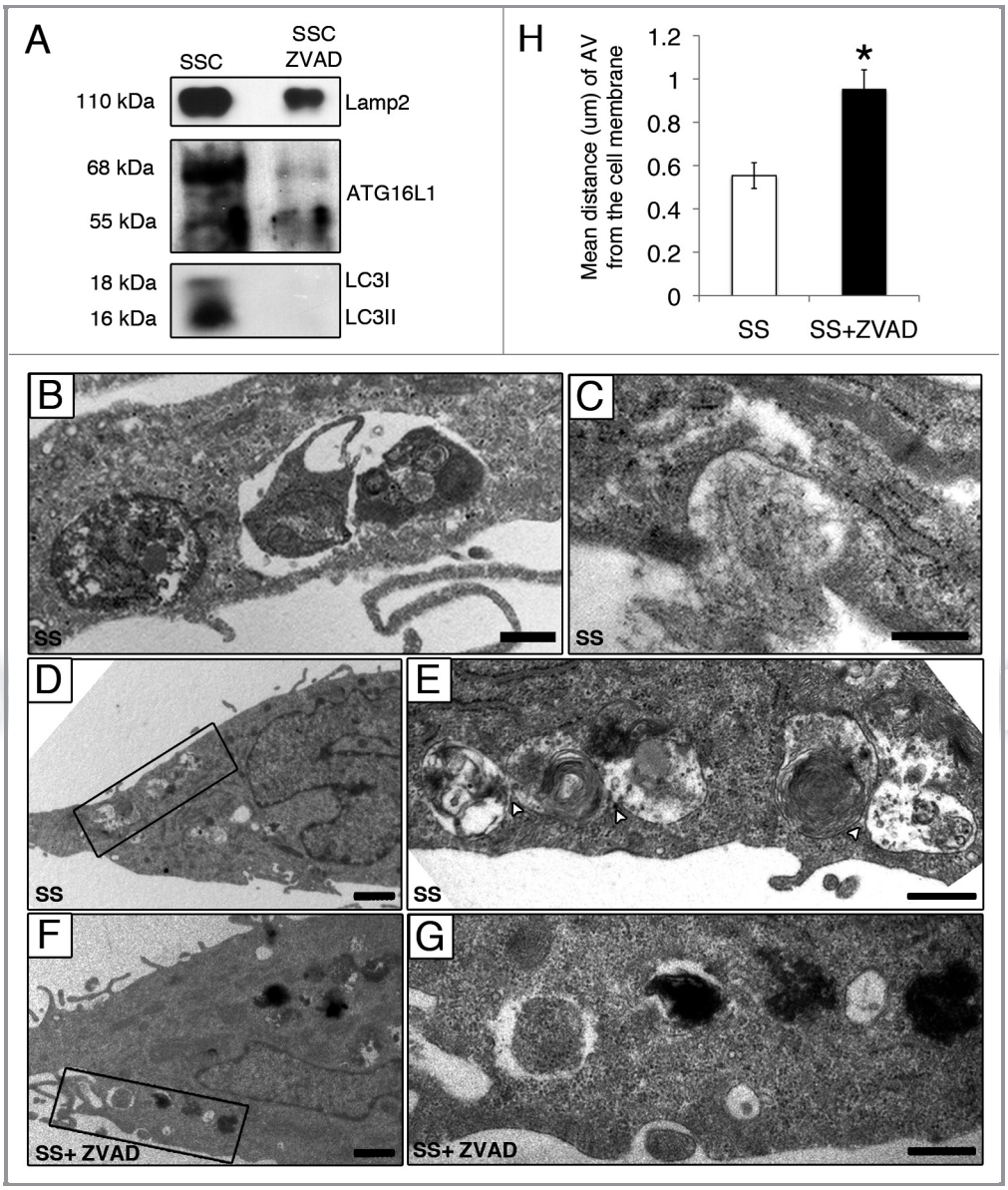

Figure 4. Caspase-dependent release of AV components during serum starvation (A) Immunoblot analysis for LAMP2, LC3-I, LC3-II and ATG16L1 in 25 ml of media conditioned by EC serum staved with vehicle DMSO (SSC) or with ZVAD-FMK 50 μM (SSC ZVAD); n = 3 for ATG16L1, LC3I and LC3-II; n = 2 for LAMP2. (B–E) Electron micrographs of EC serum starved with vehicle for 4 h showing AV near and/or interacting with the cell membrane. Scale bar: (B and C) 0.5 μm; (D) 1 μm. (E) Islet of the autophagic network in (D) located near the cell membrane; contact sites (white arrowheads). Scale bar: 0.5 μm. (F) AV in EC serum starved incubated with ZVAD-FMK 50 μM (SS + ZVAD) are located farther away from the cell membrane as opposed to AV seen in EC serum starved with vehicle (SS) (D and E). Scale bar: 1 μm. (G) Islet of the AV in (F). Scale bar: 0.5 μm. (H) Distance (μm) of AV from the cell membrane in serum-starved EC treated as in (A–G). Each AV distance was measured perpendicularly to the cell membrane in electron micrographs using ImageJ software; n = 30 cell profiles for each condition *$p < 0.001$ vs. SS.

shown that exposing human cells, including human EC, to rapamycin, a pure autophagic stimulus, is not sufficient for activation of unconventional secretion[3,29] suggesting that a caspase-dependent signal is required for export of intracellular components by unconventional secretion pathways in the early phases of apoptosis. Collectively, the present results suggest that caspase-3 activation reroutes AV toward the cell membrane, therefore facilitating their release.

The functional importance of AV release downstream of caspase activation could vary, depending on cell type and the local microenvironment. It is likely that externalization of large AV contributes to the reduction of cell volume associated with caspase-dependent apoptotic cell death.[30] Whether neighboring cells could engulf these components as a source of energy or as intercellular communication devices will be evaluated in future work. Nonetheless, our data identify new areas of crosstalk between the autophagic and apoptotic programs. In human cells and in yeast, reduction of nutrient availability favors the accumulation of AV. We propose that caspase-3 activation in stressed cells represents a molecular

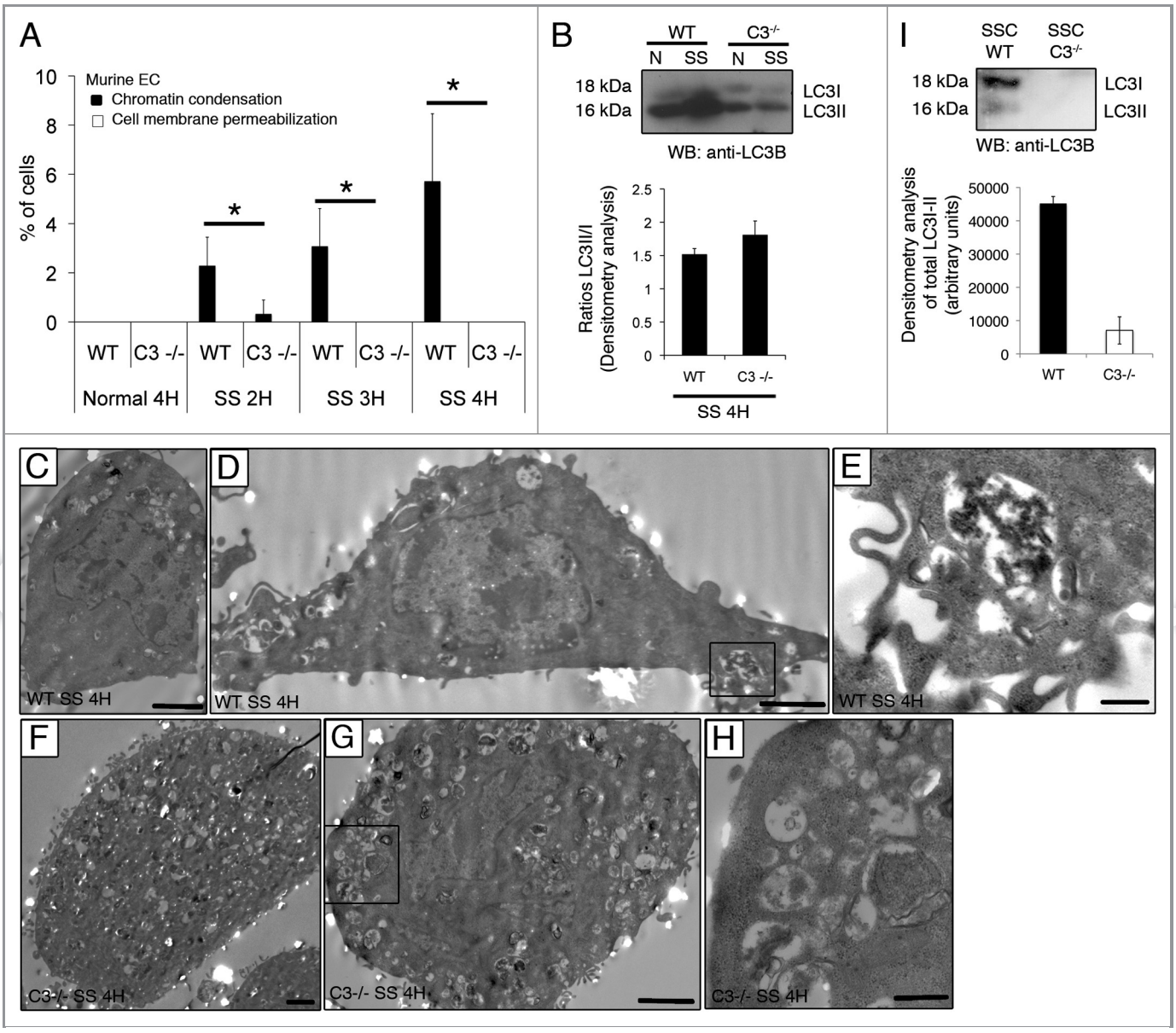

Figure 5. Caspase-3-dependent release of AV components in serum-starved murine EC. (A) Percentages of cells with chromatin condensation and cell membrane permeabilization (as evaluated by HO and PI staining) in aortic EC isolated from controls (WT) and CASP3-deficient (*C3*$^{-/-}$) mice exposed to normal medium 4 h or SS for 2–4 h. *p ≤ 0.02 vs. WT, n = 6. (B) Upper panel: Immunoblot for LC3-I/-II in EC treated as described above. *Lower panel:* densitometry analysis of LC3-II/LC3-I ratios for WT and *C3*$^{-/-}$ murine EC serum starved for 4 h. Representative of 16 independent WT mice and 6 *C3*$^{-/-}$ mice. (C–E) Electron micrographs of control murine EC (WT) exposed to SS for 4 h showing AV near and/or interacting with the cell membrane [islet in (E)]. Scale bars: (C and D) 2 μm; (E): 0.5 μm. (F–H) Electron micrographs of murine *C3*$^{-/-}$ EC exposed to SS for 4 h showing enhanced autophagic vacuolization located away from the cell membrane (islet in H) as compared with WT (E). Scale bars: (F and G) 2 μm; (H) 0.5 μm. (I) Upper panel: Immunoblot analysis for LC3-I and LC3-II in 10 ml of serum-free media conditioned by controls (SSC WT) or CASP3-deficient (SSC C3$^{-/-}$) murine EC. Lower panel: Densitometry analysis of LC3-I and LC3-II; n = 3.

switch enabling cells to re-route AV components for export purposes.

Materials and Methods

Cell culture, immunoblotting and reagents. Human umbilical vascular endothelial cells (HUVEC, Cell applications 200p-05n) were grown in endothelial cell basal medium (Lonza, CC-3121) and used at passages 2 to 4. For time course studies, HUVEC were exposed to either normal medium (N), serum-free medium (SS, RPMI, Gibco, 11875-093) SS + ZVAD-FMK (50 μM) (R&D Systems, FMK-001) for 1 to 4h or SS + vehicle (DMSO, Sigma Aldrich, D2650). Protein extracts were separated on 12% SDS-PAGE, as previously described,[13,14,31-34] and probed with rabbit polyclonal antibodies against PARP (Cell Signaling, 9542S) and LC3BI-II (Novus Biological, NB600-1384) and mouse

monoclonal Caspase-1 (Santa Cruz Biotechnology, SC56036). The LC3-II/LC3-I ratio was estimated by densitometry analysis with Image J software (NIH).

Fluorescence microscopy for quantitation of cells with chromatin condensation and cell membrane permeabilization. Fluorescence microscopy of unfixed/unpermeabilized, adherent cells, stained with Hoechst 33342 (2'-(4-ethoxyphenyl)-5-(4-methyl-1-piperazinyl)-2.5'-bi-1H-benzimidazole) (HO, Sigma Aldrich, B2261) and propidium iodide (PI, Invitrogen, P3566), was undertaken as previously described.[3-5] Briefly, cells were grown to confluence in 6-well polycarbonate culture plates (Becton-Dickinson, 3516). HO (1 μg/ml) was added for 10 min at 37°C. PI was added to a final concentration of 5 μg/ml immediately before fluorescence microscopy analysis (excitation filter l = 360–425 nm). The percentages of normal, apoptotic and necrotic cells adherent to the dishes were estimated by an investigator blinded to the experimental conditions in three random fields per condition. Apoptotic cells show increased HO fluorescence in the absence of PI positivity. Secondary and primary necrotic cells disclose PI positivity.

Electron microscopy and morphometrical evaluation. HUVEC were fixed with 1% glutaraldehyde, post-fixed with 1% osmium tetroxide and embedded in Epon according to routine techniques. The tissue sections were stained with uranyl acetate and lead citrate.[35] For quantification of the cytoplasmic surface occupied by and AV, electron micrographs were recorded for each condition and each experiment at x5,600 and x19,500. The cytoplasmic area occupied by AV was assessed in relation to the cell cytoplasm (nuclei were not included in the evaluation) with ImageJ software [area/cell profile area (μm^2)].

Confocal microscopy staining. Endothelial cells were cultivated in labtek (Thermo Fisher Scientific, 154534) as described above. Briefly, when reaching confluence, cells were treated during 4 h. Cells were then fixed 20 min on ice in 2% paraformaldehyde and permeabilized (0.1% Triton X-100 (Sigma, T9284) in PBS) 10 min. Prior to the overnight incubation in 1:30 LC3B antibody (Cell Signaling, 2775S), slides were blocked 1 h (Blocking solution: 2% goat serum (Sigma Aldrich, G9023), 1% BSA (Sigma Aldrich, A9647), 0.1% Tween20 in PBS (Sigma Aldrich, P1372). Secondary antibody goat anti-rabbit Alexa488 (Invitrogen, A11008) was used. Nuclear counterstain was visualized with DAPI (4',6-diamidino-2-phenylindole, 0.05 μg/ml, (Invitrogen, D3571). The autophagic vacuoles were visualized using a Olympus multiphoton FV-1000 MER microscope with Argon laser 488 nm line and diode laser 405 nm line. The images were taken with a UPlanSApo 60X/1.35W objective lens.

Laser confocal scanning microscopy. Alexa 488 and DAPI were imaged with Olympus FV10-MSASW software under a Olympus Laser Confocal Scanning Microscope. For Alexa 488, the 488 nm line of the Argon laser was used for excitation and emission was detected at 520 nm. DAPI imaging was visualized using a diode laser 405 nm line and emission was detected at 461 nm. Differential interference contrast (DIC) images were captured using the transmission light detector of the confocal microscope. For semiquantitative measurement of fluorescence intensities, laser, pinhole and gain settings of the confocal microscope were kept identical among treatments. LC3 puncta were counted in approximatly 50 cells/representative section of the sample in three different trials using Photoshop CS4 (Adobe System).

Characterization of the secretome produced by apoptotic EC. Serum-free media, conditioned by apoptotic or caspase-inhibited EC, were obtained as described previously.[13,14,31-34] Equal EC numbers (2.5×10^4 cells/cm^2) were set in normal medium containing either the pan-caspase inhibitor ZVAD-FMK (100 μM) or vehicle (DMSO). Then, the culture medium was changed for serum-free medium RPMI (Gibco), and the EC were serum starved for 4 h. Autophagic proteins were identified in serum-free media (0.16 ml/cm^2) conditioned by either caspase-activated EC (SSC-DMSO) or caspase-inhibited EC (SSC-ZVAD). Conditioned media were centrifuged sequentially at 1,200 g and 50,000 g to eliminate cell debris and apoptotic blebs. Two comparative proteomics approaches were used to identify the secretome released by apoptotic EC: 2D-LC-MS/MS and SDS-PAGE LC-MS/MS as previously described.[36] Protein extracts from equal volumes (25 ml) of SSC and SSC ZVAD were TCA precipitated 9:1, washed with cold acetone, heated 5 min and solubilized in sample buffer.

Experimental animals. The protocol was approved by the Comité Institutionnel de Protection des Animaux (CIPA) of the Centre Hospitalier de l'Université de Montréal (CHUM). Male and female mice, aged 6 to 8 weeks, were derived from breeding pairs of heterozygous CASP3-deficient (B6.129S1-*C3*^{tm1Flv}/J) mice obtained from Jackson Laboratory (Bar Harbor, Me). Two groups of mice were studied: homozygous CASP3-deficient (*C3*$^{-/-}$) mice and wild-type (WT) as controls. Mice were maintained in 12 h light-dark cycle and fed ad libitum. No difference was observed between male and female mice for the different parameters investigated. The genotyping of each mouse was assessed by PCR of DNA isolated from tail biopsy samples, as described on the Jackson Laboratory website.

Isolation and culture of aortic endothelial cells. Endothelial cells from the thoracic aorta were isolated by an explant technique. The thoracic aorta was gently cleaned of periadventitial fat and connective tissue and was opened longitudinally and cut into 2 mm-long segments. The aortic segments of each mouse were placed on Matrigel (Basement membrane, BD Biosciences, 354234) in a 6-well plate (2 aorta/well) and incubated in DMEM low glucose (Invitrogen,11885-092) supplemented with 10% FBS (Gibco,16000-044), 10% newborn calf serum (Gibco, 16010-159), 1% penicillin-streptomycin (Invitrogen, 151-40), 12.6 U/ml heparin (LeoPharma, 35HEIJ205), 50 μg/ml endothelial cell growth supplements (VWR, CACB356006) and 100 U/mL fungizone (Invitrogen, 15290-018) at 37°C in a 95% air/5% CO_2 incubator. The vessel segments were removed 4–5 d after the isolation and cells were detached with 50 U/ml dispase (BD Bioscience, CACB354235) and then plated onto 0.5% gelatin-coated 25-cm^2 flasks after a week in the Matrigel. The subsequent passages up to P2 were performed with 0.25% trypsin-EDTA (Invitrogen, 25300), and cells were split in a 1:4 ratio. Endothelial cells were characterized with a CD31 (Santa Cruz Biotechnology, SC1506) and VE-Cadherin (Santa Cruz Biotechnology, SC28644) immunostaining dye for each passage.

Statistical analysis. The data, expressed as mean ± standard error of the mean, were analyzed by Student's t-test (with Bonferroni correction when appropriate) or ANOVA.

Disclosure of Potential Conflicts of Interest

No potential conflicts of interest were disclosed.

Acknowledgments

This work was supported by research grants from the Canadian Institutes of Health Research to M.J.H. and M.B. (MOP-89869). M.J.H. is the holder of the Shire Chair in Nephrology, Transplantation and Renal Regeneration of the University of Montreal. I.S. is the recipient of a training fellowship from the Canadian Institutes of Health Research. We thank the J.-L. Lévesque Foundation for renewed support.

Supplemental Materials

Supplemental materials may be found here:
www.landesbioscience.com/journals/autophagy/article/19768

References

1. Lauber K, Bohn E, Kröber SM, Xiao YJ, Blumenthal SG, Lindemann RK, et al. Apoptotic cells induce migration of phagocytes via caspase-3-mediated release of a lipid attraction signal. Cell 2003; 113:717-30; PMID:12809603; http://dx.doi.org/10.1016/S0092-8674(03)00422-7
2. Bournazou I, Pound JD, Duffin R, Bournazos S, Melville LA, Brown SB, et al. Apoptotic human cells inhibit migration of granulocytes via release of lactoferrin. J Clin Invest 2009; 119:20-32; PMID:19033648
3. Sirois I, Raymond MA, Brassard N, Cailhier JF, Fedjaev M, Hamelin K, et al. Caspase-3-dependent export of TCTP: a novel pathway for antiapoptotic intercellular communication. Cell Death Differ 2011; 18:549-62; PMID:20966960; http://dx.doi.org/10.1038/cdd.2010.126
4. Longatti A, Orsi A, Tooze SA. Autophagosome formation: not necessarily an inside job. Cell Res 2010; 20:1181-4; PMID:20838417; http://dx.doi.org/10.1038/cr.2010.132
5. Liou W, Geuze HJ, Geelen MJ, Slot JW. The autophagic and endocytic pathways converge at the nascent autophagic vacuoles. J Cell Biol 1997; 136:61-70; PMID:9008703; http://dx.doi.org/10.1083/jcb.136.1.61
6. Eskelinen EL. Maturation of autophagic vacuoles in Mammalian cells. Autophagy 2005; 1:1-10; PMID:16874026; http://dx.doi.org/10.4161/auto.1.1.1270
7. Tooze J, Hollinshead M, Ludwig T, Howell K, Hoflack B, Kern H. In exocrine pancreas, the basolateral endocytic pathway converges with the autophagic pathway immediately after the early endosome. J Cell Biol 1990; 111:329-45; PMID:2166050; http://dx.doi.org/10.1083/jcb.111.2.329
8. Yi J, Tang XM. The convergent point of the endocytic and autophagic pathways in leydig cells. Cell Res 1999; 9:243-53; PMID:10628833; http://dx.doi.org/10.1038/sj.cr.7290023
9. Fader CM, Colombo MI. Autophagy and multivesicular bodies: two closely related partners. Cell Death Differ 2009; 16:70-8; PMID:19008921; http://dx.doi.org/10.1038/cdd.2008.168
10. Berg TO, Fengsrud M, Strømhaug PE, Berg T, Seglen PO. Isolation and characterization of rat liver amphisomes. Evidence for fusion of autophagosomes with both early and late endosomes. J Biol Chem 1998; 273:21883-92; PMID:9705327; http://dx.doi.org/10.1074/jbc.273.34.21883
11. Duran JM, Anjard C, Stefan C, Loomis WF, Malhotra V. Unconventional secretion of Acb1 is mediated by autophagosomes. J Cell Biol 2010; 188:527-36; PMID:20156967; http://dx.doi.org/10.1083/jcb.200911154
12. Manjithaya R, Subramani S. Role of autophagy in unconventional protein secretion. Autophagy 2010; 6:650-1; PMID:20473033; http://dx.doi.org/10.4161/auto.6.5.12066
13. Cailhier JF, Sirois I, Laplante P, Lepage S, Raymond MA, Brassard N, et al. Caspase-3 activation triggers extracellular cathepsin L release and endorepellin proteolysis. J Biol Chem 2008; 283:27220-9; PMID:18658137; http://dx.doi.org/10.1074/jbc.M801164200
14. Laplante P, Sirois I, Raymond MA, Kokta V, Béliveau A, Prat A, et al. Caspase-3-mediated secretion of connective tissue growth factor by apoptotic endothelial cells promotes fibrosis. Cell Death Differ 2010; 17:291-303; PMID:19730442; http://dx.doi.org/10.1038/cdd.2009.124
15. Huang Q, Li F, Liu X, Li W, Shi W, Liu FF, et al. Caspase 3-mediated stimulation of tumor cell repopulation during cancer radiotherapy. Nat Med 2011; 17:860-6; PMID:21725296; http://dx.doi.org/10.1038/nm.2385
16. Klionsky DJ, Abeliovich H, Agostinis P, Agrawal DK, Aliev G, Askew DS, et al. Guidelines for the use and interpretation of assays for monitoring autophagy in higher eukaryotes. Autophagy 2008; 4:151-75; PMID:18188003
17. Behrends C, Sowa ME, Gygi SP, Harper JW. Network organization of the human autophagy system. Nature 2010; 466:68-76; PMID:20562859; http://dx.doi.org/10.1038/nature09204
18. Kundu M, Thompson CB. Autophagy: basic principles and relevance to disease. Annu Rev Pathol 2008; 3:427-55; PMID:18039129; http://dx.doi.org/10.1146/annurev.pathmechdis.2.010506.091842
19. Mizushima N, Ohsumi Y, Yoshimori T. Autophagosome formation in mammalian cells. Cell Struct Funct 2002; 27:421-9; PMID:12576635; http://dx.doi.org/10.1247/csf.27.421
20. Nara A, Mizushima N, Yamamoto A, Kabeya Y, Ohsumi Y, Yoshimori T. SKD1 AAA ATPase-dependent endosomal transport is involved in autolysosome formation. Cell Struct Funct 2002; 27:29-37; PMID:11937716; http://dx.doi.org/10.1247/csf.27.29
21. Liang C, Lee JS, Inn KS, Gack MU, Li Q, Roberts EA, et al. Beclin1-binding UVRAG targets the class C Vps complex to coordinate autophagosome maturation and endocytic trafficking. Nat Cell Biol 2008; 10:776-87; PMID:18552835; http://dx.doi.org/10.1038/ncb1740
22. Jounai N, Kobiyama K, Shiina M, Ogata K, Ishii KJ, Takeshita F. NLRP4 negatively regulates autophagic processes through an association with beclin1. J Immunol 2011; 186:1646-55; PMID:21209283; http://dx.doi.org/10.4049/jimmunol.1001654
23. Tanaka Y, Guhde G, Suter A, Eskelinen EL, Hartmann D, Lüllmann-Rauch R, et al. Accumulation of autophagic vacuoles and cardiomyopathy in LAMP-2-deficient mice. Nature 2000; 406:902-6; PMID:10972293; http://dx.doi.org/10.1038/35022595
24. Keller M, Rüegg A, Werner S, Beer HD. Active caspase-1 is a regulator of unconventional protein secretion. Cell 2008; 132:818-31; PMID:18329368; http://dx.doi.org/10.1016/j.cell.2007.12.040
25. Hara-Nishimura I, Hatsugai N. The role of vacuole in plant cell death. Cell Death Differ 2011; 18:1298-304; PMID:21637288; http://dx.doi.org/10.1038/cdd.2011.70
26. Mizushima N. Autophagy: process and function. Genes Dev 2007; 21:2861-73; PMID:18006683; http://dx.doi.org/10.1101/gad.1599207
27. Romao S, Münz C. Autophagy of pathogens alarms the immune system and participates in its effector functions. Swiss Med Wkly 2011; 141:w13198; PMID:21574066
28. Amzallag N, Passer BJ, Allanic D, Segura E, Théry C, Goud B, et al. TSAP6 facilitates the secretion of translationally controlled tumor protein/histamine-releasing factor via a nonclassical pathway. J Biol Chem 2004; 279:46104-12; PMID:15319436; http://dx.doi.org/10.1074/jbc.M404850200
29. Savina A, Fader CM, Damiani MT, Colombo MI. Rab11 promotes docking and fusion of multivesicular bodies in a calcium-dependent manner. Traffic 2005; 6:131-43; PMID:15634213; http://dx.doi.org/10.1111/j.1600-0854.2004.00257.x
30. Núñez R, Sancho-Martínez SM, Novoa JM, López-Hernández FJ. Apoptotic volume decrease as a geometric determinant for cell dismantling into apoptotic bodies. Cell Death Differ 2010; 17:1665-71; PMID:20706273; http://dx.doi.org/10.1038/cdd.2010.96
31. Raymond MA, Désormeaux A, Laplante P, Vigneault N, Filep JG, Landry K, et al. Apoptosis of endothelial cells triggers a caspase-dependent anti-apoptotic paracrine loop active on VSMC. FASEB J 2004; 18:705-7; PMID:14977881
32. Laplante P, Raymond MA, Gagnon G, Vigneault N, Sasseville AM, Langelier Y, et al. Novel fibrogenic pathways are activated in response to endothelial apoptosis: implications in the pathophysiology of systemic sclerosis. J Immunol 2005; 174:5740-9; PMID:15843576
33. Laplante P, Raymond MA, Labelle A, Abe J, Iozzo RV, Hébert MJ. Perlecan proteolysis induces an alpha2beta1 integrin- and Src family kinase-dependent anti-apoptotic pathway in fibroblasts in the absence of focal adhesion kinase activation. J Biol Chem 2006; 281:30383-92; PMID:16882656; http://dx.doi.org/10.1074/jbc.M606412200
34. Soulez M, Sirois I, Brassard N, Raymond MA, Nicodème F, Noiseux N, et al. Epidermal growth factor and perlecan fragments produced by apoptotic endothelial cells co-ordinately activate ERK1/2-dependent antiapoptotic pathways in mesenchymal stem cells. Stem Cells 2010; 28:810-20; PMID:20201065; http://dx.doi.org/10.1002/stem.403
35. Bendayan M. Tech.Sight. Worth its weight in gold. Science 2001; 291:1363-5; PMID:11233453; http://dx.doi.org/10.1126/science.291.5507.1363
36. Pshezhetsky AV, Fedjaev M, Ashmarina L, Mazur A, Budman L, Sinnett D, et al. Subcellular proteomics of cell differentiation: quantitative analysis of the plasma membrane proteome of Caco-2 cells. Proteomics 2007; 7:2201-15; PMID:17549793; http://dx.doi.org/10.1002/pmic.200600956
37. Fader CM, Sánchez D, Furlán M, Colombo MI. Induction of autophagy promotes fusion of multivesicular bodies with autophagic vacuoles in k562 cells. Traffic 2008; 9:230-50; PMID:17999726; http://dx.doi.org/10.1111/j.1600-0854.2007.00677.x